Analysis of interference in attosecond transient absorption in adiabatic condition

Wenpu Dong, Yongqiang Li, Xiaowei Wang, Jianmin Yuan, and Zengxiu Zhao*

Department of Physics, College of Science, National University of Defense Technology, Changsha, Hunan 410073, China

(Received 10 March 2015; published 14 September 2015)

We simulate the transient absorption of attosecond pulses of infrared-laser-dressed atoms by considering a three-level system in the adiabatic approximation. The delay-dependent interference features are investigated from the perspective of the coherent interaction processes between the attosecond pulse and the quasiharmonics. We find that many features of the interference fringes in the absorption spectra of the attosecond pulse can be attributed to the coherence phase difference. However, the modulation signals of laser-induced sidebands of the dark state are found to be related to the population dynamics of the dark state by the dressing field.

DOI: 10.1103/PhysRevA.92.033412 PACS number(s): 32.80.Qk, 32.80.Rm, 42.50.Hz, 42.50.Md

I. INTRODUCTION

Attosecond pulses, the shortest bursts of light ever produced [1–3], allow for probing of the dynamics of bound electrons on their natural time scales, using techniques such as attosecond streaking [4,5] and electron interferometry [6,7]. With the generation of a single high-quality attosecond pulse, such pulses have been utilized as a tool for investigating the dynamic (transient) light-matter interactions on a few-femtosecond or even sublaser-cycle time scale [8–28]. Based on the pump-probe techniques, the attosecond pulses also have potential application in the study of the interference of coherent superposition states [29]. Recently, attosecond transient absorption (ATA) was applied to probe the valence electrons in atomic krypton ions generated by a controlled few-cycle laser field [8]. In the follow-up experiments, a combination of an attosecond pulse and a few-cycle laser field is used to study different atomic systems, such as helium [27,28], neon [9], argon [10], and krypton [8], identifying many interesting features in the absorption spectra. For example, one observes periodically shifted and broadened lines of low-lying states, interference-fringe phenomena, and Autler-Townes splitting of helium [27,28,30]; these phenomena are induced by pumping via an attosecond extreme ultraviolet pulse (XUV) and then probed by a delayed infrared (IR) laser pulse. Here, the information of complicated interactions between the two fields and the system is recorded in the ATA spectra.

In parallel to these experimental developments, several theoretical investigations provide fundamental insights into ATA. For the absorption of an isolated attosecond pulse in the vicinity of the helium, perturbation theory has been used to investigate the subcycle shifts and the broadened lines of $1s3p$ and $1s4p$ [11] and to yield a qualitative guide of the line shape evolution of resonant absorption lines and energy shifts of $1s^2$-$1snp$ [31]. Although perturbation theory can demonstrate the instantaneous responses of the bound electrons to the perturbing laser field, it cannot describe well the interference fringe features, the Autler-Townes splitting, and some other phenomena in the ATA spectra arising from nonlinear processes. ATA spectra are also studied via a few-level model system in the rotating-wave approximation (RWA). Although the RWA contains many effects of the interaction between the fields and the level system, the partial features of the delay-dependent interference fringes were not reproduced within this approximation [16,32]. The interference fringes in the ATA spectra of helium [27] result from the coherent quantum paths that lead to the same dipole excitation: one direct pathway is excited by the attosecond pulse and another indirect pathway is the multiphoton transition driven by the IR field. In Ref. [12], the time-dependent Schrödinger equation (TDSE) in the single-active-electron (SAE) approximation was used to analyze the effects of the coherent pathways on the interference fringes; the phases of the interference fringes are found to be dependent on the delay and the multiphoton transition driven by the IR field. However, the mechanism of the phase offset due to the multiphoton transition remains unclear.

In this paper, we focus on the delay-dependent features of the interference fringes in the ATA spectra to develop a simple picture of the ATA processes modulated by the IR dressing field. In the theoretical method, we explore the dependence of the laser-dressed dipole response on the delay, based on a three-level system that effectively models the delay-dependent interference features contained in its ATA spectra. We also take the adiabatic approximation into account, which is widely used in the stimulated Raman adiabatic passage [33–43] and here neglects the resonance-transition processes induced by the IR dressing field, allowing us to obtain an analytical solution of the dipole response. By simulating the laser-dressed dipole response of the three-level system, we find that the quasiharmonics [25,26] coherently interact with the attosecond XUV pulse at the given pulse energy. The phase differences between the quasiharmonics and the attosecond XUV pulse as a function of delay determine the periodic absorption at "$1s2p \pm 2\omega_{IR}$" in the ATA spectra.

This paper is organized as follows. In Sec. II, a brief overview of the theoretical methods involving the three-level model and the calculation of the absorption spectra is given. We present the details about describing the interference fringes by the coherence phase difference in Sec. III A, the modulation signal of the sideband of the dark state in Sec. III B, and a comparison of the simple model with the calculation of the full TDSE in the SAE approximation in Sec. III C. Finally, a short summary is given in Sec. IV.

*Corresponding author: zhao.zengxiu@gmail.com

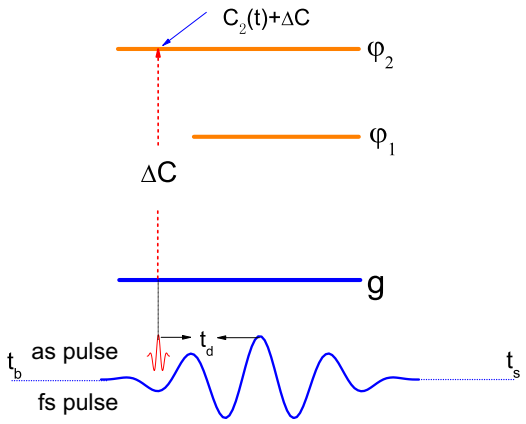

FIG. 1. (Color online) Sketch of the transition processes in the three-level system. At the delay time t_d, the attosecond pulse populates a population ΔC from the ground state to state $|\varphi_2\rangle$, bringing the probability amplitude C_2 of $|\varphi_2\rangle$ with an instant-changed ΔC.

II. METHOD

To mimic near-resonant $1s^2$-$1s2p$ XUV absorption processes in the IR-laser-dressed helium atom, we consider a three-level system interacting with a time-delayed attosecond XUV pulse and a few-cycle IR laser field. This system involves the field-free states (see Fig. 1): the ground state $|g\rangle$ and the two excited states $|\varphi_1\rangle$ and $|\varphi_2\rangle$. $|\varphi_2\rangle$ is referred to as the $1s2p$ state of helium. In addition, $|\varphi_1\rangle$, whose the dipole transition to $|g\rangle$ is prohibited, is the so-called dark state. Taking the ground-state energy as a reference, the two excited states $|\varphi_1\rangle$ and $|\varphi_2\rangle$ have energies of ω_1 and ω_2 respectively.

We consider the situation in which the weak attosecond XUV pulse has a central frequency resonant with the excitation energy ω_2, which is much larger than the frequency ω_L of the IR-dressing laser. Therefore, at each delay time t_d, the weak attosecond XUV pulse serves as a pump pulse to induce a resonant transition from the ground state to the excited state $|\varphi_2\rangle$ [16,31].

In addition we assume that $|\varphi_2\rangle$ are more strongly dipole coupled to $|\varphi_1\rangle$ than to the ground state because the transition matrix element d_{12} is larger than d_{g2}. This assumption allows us to take only the two excited states into account after the initial XUV attosecond pulse excitation during the propagation processes of the excited three-level system in the presence of the IR-dressing laser. By expanding the wave packet excited by the attosecond pulse in terms of the field-free states $\Phi = e^{-i\omega_1 t}C_1|\varphi_1\rangle + e^{-i\omega_1 t}C_2|\varphi_2\rangle$, the time-dependent Schrödinger equation for the two levels can be formulated as

$$i\frac{d}{dt}\begin{pmatrix}C_1\\C_2\end{pmatrix} = \begin{pmatrix}0 & \gamma\\ \gamma^* & \Delta\omega_{12}\end{pmatrix}\begin{pmatrix}C_1\\C_2\end{pmatrix}, \tag{1}$$

where $\gamma(t) = E(t)d_{12}$, and $E(t)$ is the IR-dressing field given by $E(t) = E_0\varepsilon(t)\cos(\omega_L t)$ with the dressing field envelope $\varepsilon(t) = \cos^2(\frac{t\pi}{\tau})$ for $t_{\rm on} \leqslant t \leqslant t_{\rm off}$, otherwise $\varepsilon(t) = 0$ with $t_{\rm on} = -\frac{\tau}{2}$, $t_{\rm off} = \frac{\tau}{2}$, and τ is the pulse duration. $\Delta\omega_{12} = \omega_2 - \omega_1$ is the resonance-transition energy between the two excited states. Atomic units are used throughout unless indicated otherwise. By diagonalizing the Hamiltonian at each instant, we have the dressed states $|\varphi_+\rangle$ and $|\varphi_-\rangle$, with the probability amplitudes of the dressed state given by

$$C_\pm = b_\pm C_1 + a_\pm C_2, \tag{2}$$

where the transform coefficients are given by $a_\pm = \omega_\pm/\sqrt{\gamma^2+\omega_\pm^2}$ and $b_\pm = \gamma/\sqrt{\gamma^2+\omega_\pm^2}$, with $\omega_\pm = \frac{1}{2}(\Delta\omega_{12} \pm \sqrt{\Delta\omega_{12}^2+4\gamma^2})$ being the energies of the dressed states $|\varphi_\pm\rangle$. The dressed energies $\omega_\pm$ are dependent on the instantaneous strengths of the dressing field. In this adiabatic model, the wave packet is strongly dressed after t_d in the presence of the IR-dressing field and maintains stable populations in the dressed states. The adiabatic model is tenable with the adiabatic condition of $|\Delta\omega_{12}| \gg \omega_L$, and the intensity of the dressing field is weak ($\leqslant 10^{14}$ W/cm^2). Assuming that at t_d, the attosecond pulse induces an instant change of the probability amplitude ΔC of $|\varphi_2\rangle$, the probability amplitudes of the two dressed states are given by $C'_\pm = \Delta C a_\pm(t_d)$. In the subsequent evolution, we have

$$C_2(t) = C'_- a_-(t)e^{-i\int_{t_d}^{t}\omega_- dt} + C'_+ a_+(t)e^{-i\int_{t_d}^{t}\omega_+ dt}, \tag{3}$$

the details of which are given in Appendix A. Based on the time evolution of the system, in particular, we focus on the dipole response from $|\varphi_2\rangle$ to the ground state with respect to the pump-probe delay. The dipole response in the time domain is given by $d(t) \approx 2\mathrm{Re}[e^{-i(t-t_d)\omega_1}C_2(t)d_{g2}]$, where we have assumed the probability amplitude of the ground state changes little and $C_2(t)$ varies as described by Eq. (3).

From the induced dipole moment, the absorption of the attosecond pulse by the system can be described by a frequency-dependent response function, following the approach in Refs. [12,13,31]:

$$S(\omega,t_d) = 2\mathrm{Im}[E^*_{atto}(\omega)d(\omega)], \tag{4}$$

where $E_{atto}(\omega)$ and d_ω are the Fourier transforms of the attosecond pulse $E_{atto}(t)$ and the dipole moment $d(t)$ with delay t_d, respectively. We use the Hanning window to eliminate the noise signal resulting from the break of the dipole moment at the ends. The response function $S(\omega,t_d)$ indicates that when the spectra phase $E_{atto}(\omega)$ of the attosecond pulse has a $\frac{\pi}{2}$ phase difference with the dipole response phase $d(\omega)$, the fields apply positive work onto the electron and the energy transfers from the pump-probe fields to the level system. When the phase difference changes by π, the reverse process occurs. The response function $S(\omega,t_d)$ describes a process of the coherent interaction between the pump-probe fields and the dipole response of the level system depending on the phase difference.

III. RESULTS AND DISCUSSION

In this section, we calculate the ATA spectra using the adiabatic model and compare them with the results from the numerical solution of the three-level TDSE. After verifying the reliability of the adiabatic model against the TDSE, we will utilize the adiabatic model to study the coherent interactions between the attosecond pulse and the delay-dependent dipole response in detail, and analyze the modulated absorption signals in ATA spectra calculated with the full TDSE in the SAE approximation.

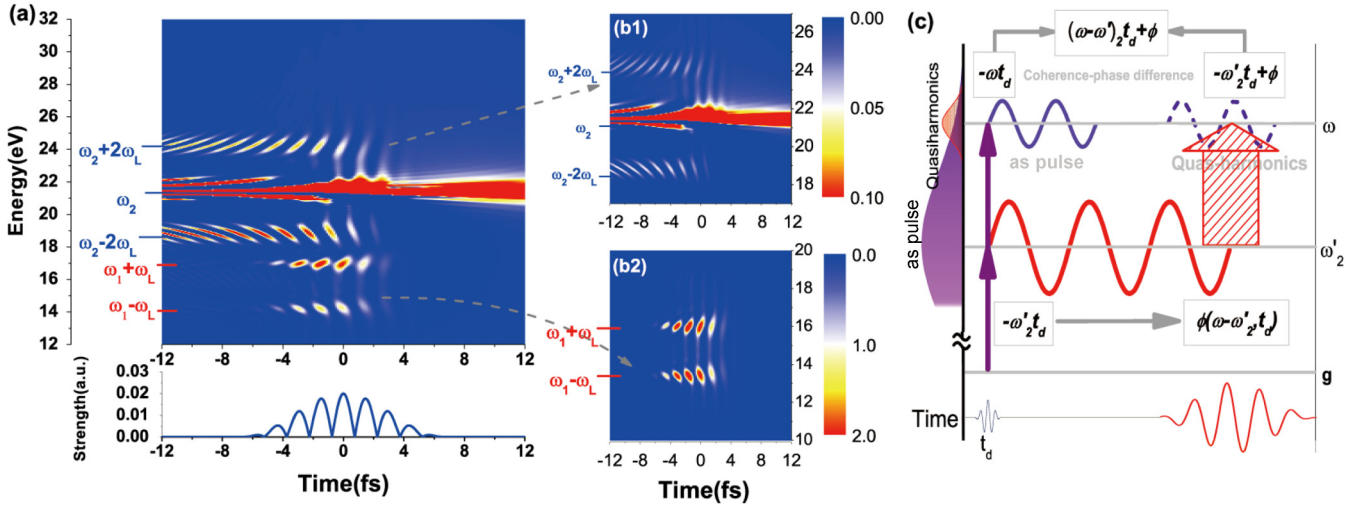

FIG. 2. (Color online) (a), (b) The response function $S(\omega,t_d)$ of the three-level system as a function of delay time. (a) Spectra from the numerical calculation of the three-level TDSE with the attosecond pulse (240 as, centered at 21.4 eV) in the presence of the dressing field (blue line, in absolute value). (b) Spectra from the calculation of the adiabatic model, shown in Eq. (3), (b1) and (b2) are the parts related to the quasiharmonics from the laser-dressed dipole responses of $|\varphi_2\rangle$ and $|\varphi_1\rangle$ to the ground state, respectively. The values of the color bars are given in atomic units. (c) Sketch of the coherence-phase difference. The interference fringes shown in (a) and (b) that are labeled as $\omega_2 \pm 2\omega_L$ result from the coherent interaction between the attosecond pulse and the quasiharmonics. The coherent phase of the quasiharmonics is associated with the effects of the attosecond pulse and the IR-dressing field. The system obtains an initial phase $-\omega_2' t_d$ excited by the attosecond pulse at the delay time, and the quasiharmonics will have an additional phase offset in the dressed processes due to the IR-dressing field.

The parameters used in the three-level model are given as follows. The ground state energy is taken as zero, and the field-free energy ω_2 of $|\varphi_2\rangle$ is 21.4 eV, corresponding to helium $1s2p$. The energy of $|\varphi_1\rangle$, $\omega_1 = 15.7$ eV, is chosen such that the resonance-transition energy between $|\varphi_1\rangle$ and $|\varphi_2\rangle$ is larger than the dressing field frequency $\omega_L = 1.38$ eV in the IR region to fulfill the adiabatic conditions. The transition matrix element from the ground state to $|\varphi_2\rangle$ is $d_{g2} = 0.3$, while the transition matrix element from $|\varphi_1\rangle$ to $|\varphi_2\rangle$ is $d_{12} = 2.7$, which is much larger than d_{g2}. To verify the validity of the adiabatic approximation, the time-dependent Schrödinger equation for the three-level system is numerically solved as well. The pulse duration of the IR-dressing field is $\tau = 13.34$ fs, with a strength of $E_0 = 0.02$ a.u. ($\approx 1.4 \times 10^{13}$ W/cm^2), while the duration of the attosecond XUV pulse with an intensity of 1×10^{10} W/cm^2, centered at 21.4 eV, is 240 as. The instant-changed ΔC that results from the attosecond pulse is set to be 0.05.

The delay-dependent response function $S(\omega,t_d)$ calculated from the numerical solution is shown in Fig. 2(a). In the figure, positive delays correspond to the attosecond pulse arriving after the center of the IR-dressing field. We observe a strong absorption line at ω_2 in the spectra, corresponding to the resonance transition from the ground state to $|\varphi_2\rangle$ induced by the attosecond pulse. The spectra also exhibit interference features, which are distributed symmetrically around $\omega_1 \pm \omega_L$ and $\omega_2 \pm 2\omega_L$, respectively. The sideband signals in the spectra around ω_1 and ω_2 are related to the quasiharmonics from the dipole response of the laser-dressed states. The spectrum of the quasiharmonics is introduced in Refs. [25,42]; here the quasiharmonics can be attributed to multiphoton-dressed processes of the IR-dressing field. The values of the sideband signals depend on the coherent interaction between the quasiharmonics and the attosecond pulse. For analysis of the quasiharmonics, we calculated the laser-dressed dipole response by the adiabatic model, as shown in Fig. 2(b), where the adiabatic model was used to calculate the dipole response for the same parameters as in Fig. 2(a). We find that the adiabatic model is in good agreement with the numerical solution of the three-level TDSE.

Because of the different energies of the quasiharmonics from different dressed states, the spectra are classified into two parts by energies $\omega_2 \pm 2\omega_L$ and $\omega_1 \pm \omega_L$, as shown in Figs. 2(b1) and 2(b2). The dipole responses of the two parts, corresponding to the transitions from the dressed states $|\varphi_\pm\rangle$ to the ground state with transition energies $\omega_1 + \omega_\pm$, are calculated by the two respective terms of $C_2(t)$ in Eq. (3): $C'_\pm a_\pm e^{-i[(t-t_d)\omega_1 + \int \omega_\pm dt]}$, for $d(t) \propto \mathrm{Re}[e^{-i(t-t_d)\omega_1} C_2(t)]$ (see Appendix A). We find that the classification of the spectra is helpful for analyzing the interference features in the spectra. In Secs. III A and III B, we will discuss the two main delay-dependent features in Fig. 2: the interference fringes from two-photon-dressed processes and the modulation signals of the laser-induced sidebands of the dark state $|\varphi_1\rangle$ at $\omega_1 \pm \omega_L$ in the spectra when the pump-probe fields overlap ($t_{\mathrm{on}} \leqslant t_d \leqslant t_{\mathrm{off}}$).

A. Delay-dependent phase of the interference fringes from two-photon-dressed processes

The interference fringes around $\omega_2 \pm 2\omega_L$ in delay-dependent absorption spectra result from the interference between direct and indirect pathways, which has been discussed previously [12,27]; we will further study the phase of the interference fringes in more detail in this section. According to the response function $S(\omega,t_d)$, the absorption of the XUV

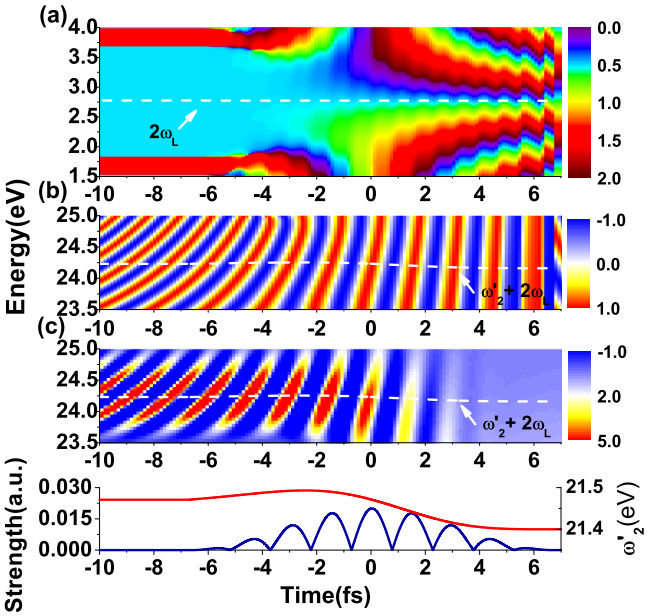

FIG. 3. (Color online) The interference fringes at $\omega_2' + 2\omega_L$. (a) The phase offset ϕ as a function of photon energy and delay. The pixel value is measured in π. (b) The interference fringes calculated by Eq. (7), where ϕ is given in (a), and ω_2' is shown as the red line. (c) The interference fringes are the same as in Fig. 2(a).

field pulse could be regarded as a coherent interaction process depending on the phase difference between the XUV field pulse and the laser-dressed dipole response of the atom. In the following discussion, we extract the quasiharmonics from the laser-dressed dipole response, which can contribute to the coherent interaction processes around the energy $\omega_2 \pm 2\omega_L$. Therefore, the delay-dependent phase of the interference fringes is discussed by the coherence-phase difference between the attosecond XUV pulse and the quasiharmonics.

The coherence-phase difference between the attosecond XUV pulse and the quasiharmonics from two-photon-dressed processes is required for describing the response function $S(\omega,t_d)$ around $\omega_2 + 2\omega_L$ in the ATA spectra. The sketch map of generation processes of the coherence-phase difference is shown in Fig. 2(c). The spectral phase of the attosecond XUV pulse can be obtained by Fourier transform. To obtain the phase of the dipole response, we assume there is a $\frac{\pi}{2}$ phase difference between the attosecond pulse and the dipole response at the resonance-transition energy ω_2; this assumption is reasonable for the resonance absorption by the system. However, a modification is required on the resonance-transition energy ω_2 for the as-stark shift by the IR-dressing field [11,31]. We consider the effect of the time-averaged shift energy $\delta\omega$, over the part of the duration of the IR-dressing field pulse arriving after t_d. In this case, the resonance-transition energy is approximated by

$$\omega_2' \approx \omega_2 + \delta\omega(t_d), \tag{5}$$

where $t_{on} < t_d \leqslant t_{off}$, and the shift energy $\delta\omega(t_d)$ is given in Eq. (B2) according to the adiabatic model (see Appendix B). The modified energy ω_2' as a function of delay is shown in the red line of Fig. 3. The excited dipole response propagates in the delay period, which causes a phase difference $(\omega - \omega_2')t_d$ for the different frequencies. After the delay period, the excited dipole is dressed by the dressing field and generates quasiharmonics with energy $\omega_2' \pm 2\omega_L$. The quasiharmonics, corresponding to the effects of the two-photon of the IR-dressing field, have a phase difference of $\phi - \frac{\pi}{2}$ with the dipole response at ω_2', where the phase offset ϕ is given by (see details in Appendix B)

$$\phi(\omega,t_d) = \arg\left[\int_{-\infty}^{+\infty} \theta(t) e^{-i\omega t} dt\right]. \tag{6}$$

The phase offset ϕ arising from the coupling processes between the IR-dressing field and the system is shown in Fig. 3(a).

The coherence-phase difference is $(\omega - \omega_2')t_d + \phi$, and then the response function $S(\omega,t_d)$ can be given as a function of the coherence-phase difference, approximately:

$$S(\omega,t_d) \propto \sin\left[(\omega - \omega_2')t_d + \phi(\omega - \omega_2',t_d)\right]. \tag{7}$$

With this function, we can describe the delay-dependent interference fringes, as shown in Fig. 3. The phase offsets $\phi(\omega,t_d)$ and $\omega_2'(t_d)$ are unchanged when the attosecond pulse arrives before the IR-dressing field $t_d < t_{on}$, and the shapes of the interference fringes follow the hyperbolic lines. When $t_{on} < t_d \leqslant t_{off}$ the pump and probe fields are overlapped, the fringe shapes are changed dramatically, and the slope of the fringes will saturate when delay time approaches the end of the dressing field. The changes in the fringe shapes, which are dependent on the coherence-phase difference as a function of delay and energy, are obviously indicated by the variation of the phase offset $\phi(\omega,t_d)$, especially before the peak of the IR-dressing field. We also find that $\phi(2\omega_L) = \frac{\pi}{2}$ is independent of the delay time, which indicates that the two-photon-dressed processes of the dressing field vary little with respect to delay. This result indicates that the strong absorption of the attosecond pulse at $\omega_2' + 2\omega_L$ occurs at the peak times of the dressing field. This strong absorption can be utilized to calibrate the position of the interference fringes in the delay-dependent spectra.

We remark here that the adiabatic model captures much of the three-level system dynamics with the resonance-transition energy $\Delta\omega_{12}$ larger than the photon energy ω_L of the dressing field; however, the dynamics of the adiabatic model cannot include transition processes between the dressed states. In fact, the transition processes cannot be ignored when $|\Delta\omega_{12}| \leqslant \omega_L$, which may affect the laser-dressed dipole response phase and the interference fringes in the ATA spectra as well. Although the adiabatic model is not adequate, it provides a quantitative description of the interference features from the laser-dressed system in ATA.

B. Modulation signals on the sidebands from one-photon-dressed processes

Compared to the two-photon-dressed processes in Sec. III A, the modulations of the sidebands with one-photon coupled processes demonstrate different interference-fringe features. In this section, we focus on the modulation of the spectra of the laser-induced sidebands with energy $\omega_1 \pm \omega_L$ in the spectra, corresponding to one-photon-dressed processes,

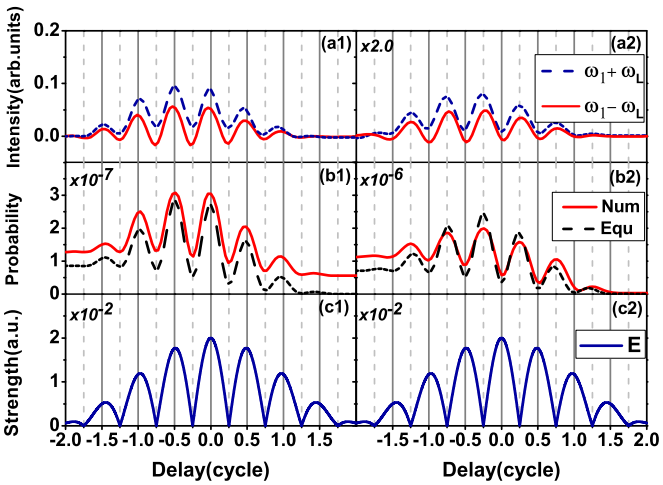

FIG. 4. (Color online) Comparison of the modulation phase of the sidebands of state $|\varphi_1\rangle$ with $|\Delta\omega_{12}| \gg \omega_L$ [left, (a1)–(c1)] and $|\Delta\omega_{12}| \ll \omega_L$ [right, (a2)–(c2)]. $\Delta\omega_{12}$ is changed by setting the energy value of $|\varphi_1\rangle$ with $\omega_1 = 15.7$ and 21.0 eV. The delay time is given in the cycle time of the dressing field for clarity. (a) The area of the sideband signal [integrated over the range of 0.5 eV with the center energy at the sideband peak intensity in Fig. 2(a)] as a function of the delay time. (b) The average occupancy $\overline{|C_1|^2}$ given in Eq. (8) as a function of the delay time. Red lines with the label "Num" are numerically solved using the TDSE, and black dash-dot line with the label "Equ" are based on Eq. (9). (c) Absolute value of the dressing field strength as a function of the delay time for reference.

as shown in Fig. 2(b2). Actually, the sidebands are strongly affected by the pump probability of the dressed state $|\varphi_-\rangle$ excited by the attosecond pulse.

In the adiabatic model, the resonance absorption of the attosecond pulse at $\omega_1 \pm \omega_L$ is related to the occupation probability of the $|\varphi_-\rangle$. Considering the relations between the dressed states and the field-free states from Eq. (2), the changes in the occupancy of $|\varphi_1\rangle$ reflect the occupation probabilities of $|\varphi_-\rangle$. Thus, the intensity of the sidebands can be indicated by the average of $|\varphi_1\rangle$ occupancy over the dressing field pulse duration:

$$\overline{|C_1|^2} = \frac{1}{t_{\rm off} - t_{\rm on}} \int_{t_{\rm on}}^{t_{\rm off}} |C_1(t)|^2 dt, \tag{8}$$

where $\overline{|C_1|^2}$ is the average of occupation probability of $|\varphi_1\rangle$ over the dressing field pulse duration. The modulation signals of the sidebands of $|\varphi_1\rangle$ can be indicated by the parameter $\overline{|C_1|^2}$, as shown in Fig. 4, where the lines of the dressing field strength, average occupancy $\overline{|C_1|^2}$, and the sidebands signals demonstrate the identical modulations. Here, under the adiabatic condition $|\Delta\omega_{12}| \gg \omega_L$, the transition to $|\varphi_1\rangle$ depends on the coupling between the field-free states by the dressing field. The strength of the dressing field is strong at t_d and then strongly couples the field-free states, which enables the transition to $|\varphi_1\rangle$ with "XUV+IR" processes to occur more easily. As a result, the population of $|\varphi_1\rangle$ varies periodically with respect to the delay time as the changes of strengths of the dressing field at the pump times of the attosecond pulse.

We also calculate the case with $|\Delta\omega_{12}| \ll \omega_L$. Under this condition, the strong Rabi flopping between the bound states induced by the dressing field will contribute to the dipole oscillation of the system. The Rabi flopping causes the oscillation of the populations of the dressed states and results in the nonadiabatic processes. The calculations of this case are shown in Fig. 4. We find that there is a π phase difference compared to the lines from the adiabatic case from Fig. 4.

The π phase shift of $\overline{|C_1|^2}$ in nonadiabatic processes is related to the effects of the dressing field after t_d, which cause the strong Rabi flopping. For clarity, we calculate the average occupancy $\overline{|C_1|^2}$ by only considering the transition from $|\varphi_2\rangle$ to $|\varphi_1\rangle$ with the effects of the dressing field. Here, we assume that the dressing field causes little change of the probability amplitude of $|\varphi_2\rangle$ with the off-resonant condition, such that $C_2(t) \approx \Delta C \exp[-i(t - t_d)\Delta\omega_{12}]$. Then, the average occupancy $\overline{|C_1|^2}$ is (see Appendix C)

$$\overline{|C_1|^2} \approx \frac{(t_{\rm off} - t_d)\eta^2\varepsilon(t_d)^2}{t_{\rm off} - t_{\rm on}}\left[\omega_L^2 \sin^2(\omega_L t_d) + \Delta\omega_{12}^2 \cos^2(\omega_L t_d)\right] + \eta^2 \int_{t_d}^{t_{\rm off}} \varepsilon(t)^2 \frac{\omega_L^2 + \Delta\omega_{12}^2}{2} dt, \tag{9}$$

where $t_{\rm on} \leqslant t_d \leqslant t_{\rm off}$. The results calculated using Eq. (9) fit well with the numerical results in the off-resonant conditions, as shown in Fig. 4. The π phase difference validates the changes in the effects of the dressing field under the two off-resonant conditions. Note that the signals of the sidebands of $|\varphi_1\rangle$ are sensitive to $\overline{|C_1|^2}$ in Fig. 4, even though the modulation changed with the different conditions. This result demonstrates that the modulation phases of the sideband signals with one-photon-dressed processes are also affected by the following dressed processes after the system excited by the attosecond pulse.

C. Comparisons with the TDSE in the SAE approximation

In this section, the response function $S(\omega,t_d)$ of helium calculated with the TDSE in the SAE approximation is described. We compare the calculations with the three-level model, which demonstrates that the simple model qualitatively agrees with the basic features of the spectra. We will analyze the interference fringes and the laser-induced sidebands in detail.

Figure 5 shows the response function $S(\omega,t_d)$ calculated via the full TDSE in the SAE approximation. The calculation recovers many features observed in the ATA experiments [27], such as interference fringes, Autler-Townes splitting of the $2p$ level, and laser-induced sidebands from $1sns$ and $1snd$ dressed up or down one-photon energy. The IR-dressing field is the same shape as the dressing field used in the calculation before, with an intensity of 2×10^{12} W/cm^2, which is not strong enough to excite helium out of the ground state. The 240-as XUV has a central frequency of 22 eV and an intensity of 1×10^{11} W/cm^2, such that the bandwidth of the attosecond pulse overlaps all of the singly excited and low-energy continuum states of the helium atom. To describe the helium atom within the SAE approximation, we employ a one-electron model potential, which is given in [44]. The model potential

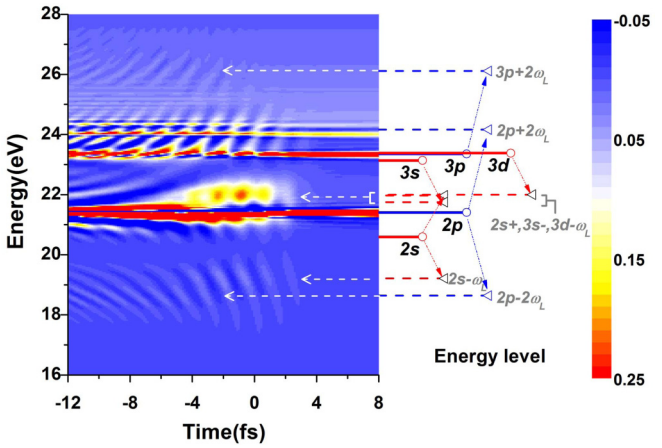

FIG. 5. (Color online) The response function spectra calculated with the TDSE in the SAE approximation as a function of delay time. Parts of the singly excited states are shown on the right side, where the dashed lines indicate the energy levels are up or down by one- or two-photon energy.

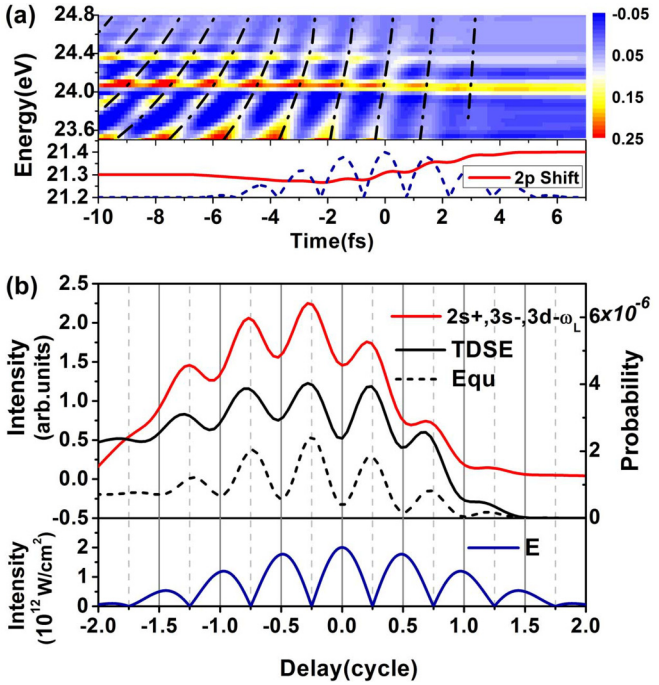

FIG. 6. (Color online) Comparison of the calculations from the TDSE in the SAE approximation and the three-level model. (a) The interference fringes appeared in the spectral region near $1s2p(21.4\text{ eV}) + 2\omega_L$. The black dash-dot lines are from the three-level model, where the energy shifts of $1s2p$ are shown by red line under the spectra. The IR intensity oscillations are shown by the blue dashed line. (b) The modulations of the laser-induced sidebands signals as a function of the delay time. The area of the sideband signal (integrated over the range of 0.5 eV with the center energy at the sideband peak (22.1 eV) intensity in Fig. 5) is indicated by the red line, which is attributed to the united effects of the sidebands of $1s2s$, $1s3s$, and $1s3d$. The average-occupancy lines from the full TDSE (black line) and from three-level model (black dashed line). The intensity of the IR field (blue line).

reproduces the ionization potential $I_p = 24.9$ eV, and the resonance-transition energy between $1s^2$ and $1s2p$ is 21.4 eV.

Figure 5 shows strong interference fringes at the energy "$2p + 2\omega_L$," where the energy is related to the quasiharmonics from $1s2p$ dressed two-photon energy. The quasiharmonics overlaps the $1snp$ states ($n \geqslant 4$), which suggests the indirect pathway from $1s2p$ to $1snp$. The indirect pathway interferes with the direct pathway from $1s^2$ to $1snp$ by the attosecond pulse, which induces the absorption lines of $1s^2$-$1snp$ to exhibit interference fringes. The spectra also show interference fringes above the ionization threshold (24.9 eV) and below the $1s2s$ state, with similar fringes being observed experimentally [27], where there is no underlying bound state. These interference fringes are discussed in Sec. III A. Both types of the interference fringes are related to the same coherent processes between the attosecond pulse and the quasiharmonics, so we can describe the fringes using the three-level model.

We focus on interference fringes around the energy "$2p + 2\omega_L$," as shown in Fig. 6(a). For comparison with the results from the full TDSE, the peak positions of the interference fringes calculated with the three-level model are indicated by the black dash-dot lines. The peak positions correspond to the coherence-phase differences $2n\pi + \frac{\pi}{2}$ (n is integer) in Eq. (7), which are related to the shift energy ω_2' of the $1s2p$ level and the phase offset ϕ from the two-photon-dressed processes. In the calculation of the full TDSE, the $1s2p$ state is shifted by coupling to nearby bound states, which was discussed in Ref. [31]. We follow the calculation (detail in Appendix B) and determine the average shift of $1s2p$ as a function of delay [red line in Fig. 6(a)]. The energy shift of $1s2p$ is negative, such that the $1s2p$ level will move together with its quasiharmonics downwards. The phase offset ϕ is calculated using the adiabatic model by Eq. (6). Figure 6(a) shows a good agreement of the slopes of the fringes between the full TDSE and the three-level model. The slopes of the fringes trend to saturate for $t_d > 0$, reflecting the effects of the phase offset ϕ. The adiabatic model predicts the variation in the phase offset well, because the interference fringes are strongly affected by the nearby bound states, such as $1s3s$ and $1s3d$ (shown in Fig. 5). The dipole couplings between these bound states and $1s2p$ approximately satisfy the adiabatic condition.

The modulation of the laser-induced sidebands are observed around the energy of 22.1 eV in the spectra (Fig. 5), where the sidebands of $2s + \omega_L$, $3s - \omega_L$, and $3d - \omega_L$ are approximately that energy. The three laser-induced sidebands join into a single sideband because the short dressing field broadens the bandwidths of the sidebands and they overlap each other. We analyze the modulation of the integral signal over the range of 0.5 eV with the center energy at 22.1 eV in the spectra in Fig. 5, with the results indicated by the red line [shown in Fig. 6(b)]. We also calculate the average occupancies of the $1s2s$, $1s3s$, and $1s3d$ states within the full TDSE at one delay time and add the values of the three states, and then obtain a line as a function of delay [black line shown in Fig. 6(b)]. In Fig. 6(b), the average-occupancy line shows the same modulations with the sideband signals (red line), which demonstrates the laser-induced sidebands at 22.1 eV are mainly attributed to the $1s2s$, $1s3s$, and $1s3d$ states. We

compare the average occupancy line with the oscillations of the field intensity and find that the modulations of the average occupancy are in accord with the case of $|\Delta\omega_{12}| \ll \omega_L$ discussed in Sec. III B [black dashed line in Fig. 6(b)]. This agreement is because the $1s2s$, $1s3s$, and $1s3d$ states are strongly coupled to the closest np or nf states by the dressing field. The transition energy between the coupled states is much less than the photon energy ω_L, so the modulations are in agreement with the calculation in the off-resonant condition.

Note that the response function can hardly provide an exact description to what is observed in the ATA experiments for the effect of propagation in the medium, although, when the gas medium is of low density, the calculation is a good guide [31]. However, according to the comparisons between the full TDSE and the three-level model, the simple model could be helpful as a guide to the delay-dependent phenomena in ATA spectra.

IV. SUMMARY

In conclusion, we have investigated the interference features of the ATA spectra using the three-level system in the presence of both the IR-dressing field and a delayed attosecond pulse. We analysed the interference fringes using the adiabatic model and compared the model results with the numerical solution of the three-level TDSE. The model revealed the qualitative relationship between the interference fringes and the dressing field. Our results demonstrated that the coherent interaction processes between the attosecond pulse and the quasiharmonics from the two-photon-dressed processes could produce the interference fringes observed in the ATA spectra. The interference fringes are determined by the coherence phase difference, which is dependent on the pump-probe delay time and the energy-shift processes driven by the dressing field. We also demonstrated that the signals of the laser-induced sidebands around the dark level in the ATA spectra is associated with the average occupancies of the dark state over the duration of the dressing field, which are modulated periodically with respect to the delay time. Moreover, we found that if the photon energy of the dressing field strides across the resonance-transition energy between the bound states, then the laser-induced sideband signals as a function of delay will have a π phase jump. This result showed the modulations of the sideband signals in the ATA spectra are also affected by the following processes dressed by the IR laser field after the attosecond pulse. Through a comparison with the calculation using the full TDSE in the SAE approximation, the three-level model with suitable conditions was found to provide good insight into the ATA processes, such as the two-photon-dressed processes and the oscillated occupancies of the dark states induced by the dressing field.

ACKNOWLEDGMENTS

This work was supported by the National Basic Research Program of China (973 Program) under Grant No. 2013CB922203, National Natural Science Foundation of China (Grants No. 11374366 and No. 11274383), and the National High-Tech ICF Committee of China.

APPENDIX A: SOLUTIONS OF ADIABATIC MODEL

With the transform relationship between the dressed states and the dark states $|\varphi_1\rangle$ from Eq. (2), Eq. (1) can be expressed in the dressed states representation:

$$\begin{aligned} i\frac{dC_-}{dt} &= \omega_- C_- - i\beta_+ C_+, \\ i\frac{dC_+}{dt} &= \omega_+ C_+ - i\beta_- C_-. \end{aligned} \tag{A1}$$

When the adiabatic condition is satisfied, i.e., $|\Delta\omega_{12}| \gg \omega_L$, and the intensity of the dressing field is weak ($\leqslant 10^{14}$ W/cm^2), such that $|\beta_\pm| = |\frac{\gamma'\Delta\omega_{12}}{4\gamma^2+\Delta\omega_{12}^2}| \ll 1$, then the system is evolving adiabatically [40,41]. In the adiabatic approximation, we take $|\beta_\pm| = 0$.

Assuming at t_d, the attosecond pulse induces an instantaneous change in the probability amplitude ΔC of $|\varphi_2\rangle$, the probability amplitudes of the two dressed states are given by $C'_\pm = \Delta C a_\pm(t_d)$. In the subsequent evolution, this equation has the following solutions:

$$\begin{aligned} C_2(t) &= C'_- a_-(t) \exp\left(-i\int_{t_d}^{t} \omega_- dt\right) \\ &\quad + C'_+ a_+(t) \exp\left(-i\int_{t_d}^{t} \omega_+ dt\right), \\ C_1(t) &= C'_- b_-(t) \exp\left(-i\int_{t_d}^{t} \omega_- dt\right) \\ &\quad + C'_+ b_+(t) \exp\left(-i\int_{t_d}^{t} \omega_+ dt\right). \end{aligned} \tag{A2}$$

In particular, this paper focuses on the dipole response from $|\varphi_2\rangle$ to the ground state with respect to the pump-probe delay. The dipole response in the time domain is given by $d(t) \approx 2\mathrm{Re}[e^{-i(t-t_d)\omega_1} C_2(t) d_{g2}]$, where the following assumptions are made: the probability amplitude of the ground state changes little, and $C_2(t)$ involves no transition from the ground state before t_d and then varies as described by Eq. (A2) after t_d.

APPENDIX B: PHASE OF THE QUASIHARMONICS WITH TWO-PHOTON-DRESSED PROCESSES

With the adiabatic model, $C'_+ a_+ e^{-i[(t-t_d)\omega_1 + \int \omega_+ dt]}$ in Eq. (3) contributes to the dipole response with two-photon-dressed processes. Under the adiabatic condition, $\omega_+ \approx \Delta\omega_{12}$, this allows for an approximation of this term in Eq. (3):

$$\begin{aligned} &C'_+ a_+(t) e^{-i[(t-t_d)\omega_1 + \int_{t_d}^{t} \omega_+ dt']} \\ &\approx C'_+ e^{-i[(t-t_d)\omega_2 + \int_{t_d}^{t} \frac{\gamma^2(t')}{\Delta\omega_{12}} dt']} \\ &\approx C'_+ e^{-i[(t-t_d)\omega_2 + \delta\theta(t)]} e^{-i\theta(t)}, \end{aligned} \tag{B1}$$

where the $\delta\omega$ and $\theta(t)$ are defined as

$$\begin{aligned} \delta\theta(t) &= \int_{t_d}^{t} \frac{[E_0 d_{12}\varepsilon(t')]^2}{2\Delta\omega_{12}} dt', \\ \theta(t) &= \int_{t_d}^{t} \frac{\gamma^2(t')}{\Delta\omega_{12}} dt' - \delta\theta(t). \end{aligned}$$

The average of the shift energy over $[t_d, t_{\rm off}]$ is given by

$$\delta\omega(t_d) = \frac{\delta\theta(t_{\rm off})}{t_{\rm off} - t_d}, \tag{B2}$$

For extracting the phase of the quasiharmonics with two-photon-dressed processes from the dipole response, the factor $e^{-i\theta(t)}$ is expanded in a Taylor series with the condition $|\theta(t)| < 1$:

$$e^{-i\theta(t)} \approx 1 - i\theta(t), \tag{B3}$$

where only the first two terms are retained and the high-order terms, including high-order effects of the IR-dressing field, are neglected. The two terms of Eq. (B3) are related to the dipole response from $|\varphi_2\rangle$ to the ground, and the quasiharmonics with two-photon-dressed processes of $|\varphi_2\rangle$. The quasiharmonics have a phase difference $(\phi - \frac{\pi}{2})$ with the dipole response of the level $|\varphi_2\rangle$, where $\frac{\pi}{2}$ comes from the factor i in Eq. (B3). According to Eq. (B3), the phase offset ϕ is given by

$$\phi(\omega, t_d) = \arg\left[\int_{-\infty}^{+\infty} \theta(t) e^{-i\omega t} dt\right], \tag{B4}$$

where "arg" is the function that extracts the argument of the value.

In the calculation of the ac stark shifts of the $1s2p$ level, we use the second-order perturbation theory introduced by Ref. [31]. These shifts in $1s2p$ are given by

$$\delta\varepsilon'_{1s2p}(t) = \begin{cases} E(t)^2 \sum \frac{\omega_n |\mu_n|^2}{\omega_n^2 - \omega_L^2}; & ||\omega_n| - \omega_L| \geqslant \Delta\omega_L, \\ E(t)^2 \sum \frac{\omega_n |\mu_n|^2}{(\omega_n \mp \omega_L)\Delta\omega_L}; & ||\omega_n| - \omega_L| < \Delta\omega_L, \end{cases} \tag{B5}$$

where $\omega_n = \varepsilon_n - \varepsilon_{1s2p}$ and μ_n are the energy difference and the dipole transition matrix element, respectively, of all intermediate states n that are dipole coupled to $1s2p$. $\Delta\omega_L$ is the IR-dressing field bandwidth: in our calculation $\Delta\omega_L = 0.5$ eV. Thus, according to Eq. (B2), the average shift of $1s2p$ is given by

$$\delta\omega'_{1s2p}(t_d) = \frac{1}{t_{\rm off} - t_d} \int_{t_d}^{t_{\rm off}} \delta\varepsilon'_{1s2p}(t') dt'. \tag{B6}$$

APPENDIX C: OCCUPANCY OF $|\varphi_1\rangle$ WITH THE OFF-RESONANT CONDITION

Considering the transition from $|\varphi_2\rangle$ to $|\varphi_1\rangle$, assuming that the dressing field causes little change in the probability amplitude of $|\varphi_2\rangle$ with the off-resonant condition, such that $C_2(t) \approx \Delta C \exp[-i(t - t_d)\Delta\omega_{12}]$, the probability amplitude of the field-free state $|\varphi_1\rangle$ is

$$C_1(t) = -i\Delta C \int_{t_d}^{t} E(t') d_{12} e^{-i(t'-t_d)\Delta\omega_{12}} dt'. \tag{C1}$$

Then according to Eq. (8), the integral average $\overline{|C_1|^2}$ is

$$\overline{|C_1|^2} \approx \frac{(t_{\rm off} - t_d)\eta^2 \varepsilon(t_d)^2}{t_{\rm off} - t_{\rm on}} \left[\omega_L^2 \sin^2(\omega_L t_d) + \Delta\omega_{12}^2 \cos^2(\omega_L t_d)\right] + \eta^2 \int_{t_d}^{t_{\rm off}} \varepsilon(t)^2 \frac{\omega_L^2 + \Delta\omega_{12}^2}{2} dt, \tag{C2}$$

where $\eta = \frac{E_0 d_{12} \Delta C}{\Delta\omega_{12}^2 - \omega_L^2}$, $t_{\rm on} \leqslant t_d \leqslant t_{\rm off}$.

[1] P. M. Paul, E. S. Toma, P. Breger, G. Mullot, F. Augé, P. Balcou, H. G. Muller, and P. Agostini, Science **292**, 1689 (2001).

[2] M. Hentschel, R. Kienberger, C. Spielmann, G. A. Reider, N. Milosevic, T. Brabec, P. Corkum, U. Heinzmann, M. Drescher, and F. Krausz, Nature (London) **414**, 509 (2001).

[3] R. Kienberger, E. Goulielmakis, M. Uiberacker, A. Baltuska, V. Yakovlev, F. Bammer, A. Scrinzi, T. Westerwalbesloh, U. Kleineberg, U. Heinzmann, M. Drescher, and F. Krausz, Nature (London) **427**, 817 (2004).

[4] J. Itatani, F. Quéré, G. L. Yudin, M. Y. Ivanov, F. Krausz, and P. B. Corkum, Phys. Rev. Lett. **88**, 173903 (2002).

[5] F. Krausz and M. Ivanov, Rev. Mod. Phys. **81**, 163 (2009).

[6] T. Remetter, P. Johnsson, J. Mauritsson, K. Varjú, Y. Ni, F. Lépine, E. Gustafsson, M. Kling, J. Khan, R. López-Martens, K. J. Schafer, M. J. J. Vrakking, and A. L'Huillier, Nat. Phys. **2**, 323 (2006).

[7] J. Mauritsson, T. Remetter, M. Swoboda, K. Klnder, A. L'Huillier, K. J. Schafer, O. Ghafur, F. Kelkensberg, W. Siu, P. Johnsson, M. J. J. Vrakking, I. Znakovskaya, T. Uphues, S. Zherebtsov, M. F. Kling, F. Lépine, E. Benedetti, F. Ferrari, G. Sansone, and M. Nisoli, Phys. Rev. Lett. **105**, 053001 (2010).

[8] E. Goulielmakis, Z. H. Loh, A. Wirth, R. Santra, N. Rohringer, V. S. Yakovlev, S. Zherebtsov, T. Pfeifer, M. A. Azzeer, M. F. Kling, S. R. Leone, and F. Krausz, Nature (London) **466**, 739 (2010).

[9] X. W. Wang, M. Chini, Y. Cheng, Y. Wu, X. M. Tong, and Z. Chang, Phys. Rev. A. **87**, 063413 (2013).

[10] H. Wang, M. Chini, S. Chen, C. H. Zhang, Y. Cheng, F. He, Y. Wu, U. Thumm, and Z. Chang, Phys. Rev. Lett. **105**, 143002 (2010).

[11] M. Chini, B. Zhao, H. Wang, Y. Cheng, S. X. Hu, and Z. Chang, Phys. Rev. Lett. **109**, 073601 (2012).

[12] S. Chen, M. Wu, M. B. Gaarde, and K. J. Schafer, Phys. Rev. A **87**, 033408 (2013).

[13] M. B. Gaarde, C. Buth, J. L. Tate, and K. J. Schafer, Phys. Rev. A **83**, 013419 (2011).

[14] M. Holler, F. Schapper, L. Gallmann, and U. Keller, Phys. Rev. Lett. **106**, 123601 (2011).

[15] A. Wirth, M. T. Hassan, I. Grguraš, J. Gagnon, A. Moulet, T. T. Luu, S. Pabst, R. Santra, Z. A. Alahmed, A. M. Azzeer, V. S. Yakovlev, V. Pervak, F. Krausz, and E. Goulielmakis, Science **334**, 195 (2011).

[16] A. N. Pfeiffer and S. R. Leone, Phys. Rev. A **85**, 053422 (2012).

[17] W. C. Chu, S. F. Zhao, and C. D. Lin, Phys. Rev. A **84**, 033426 (2011).

[18] M. Schultze, E. M. Bothschafter, A. Sommer, S. Holzner, W. Schweinberger, M. Fiess, M. Hofstetter, R. Kienberger, V. Apalkov, V. S. Yakovlev, M. I. Stockman, and F. Krausz, Nature (London) **493**, 75 (2013).

[19] L. Argenti, Á. Jiménez-Galán, C. Marante, C. Ott, T. Pfeifer, and F. Martín, Phys. Rev. A **91**, 061403(R) (2015).
[20] Z. Q. Yang, D. F. Ye, T. Ding, T. Pfeifer, and L. B. Fu, Phys. Rev. A **91**, 013414 (2015).
[21] J. M. Ngoko Djiokap, S. X. Hu, W.-C. Jiang, L.-Y. Peng, and A. F. Starace, Phys. Rev. A **88**, 011401(R) (2013).
[22] T. Zuo, S. Chelkowski, and A. D. Bandrauk, Phys. Rev. A **49**, 3943 (1994).
[23] L. Jönsson, J. Opt. Soc. Am. B **4**, 1422 (1987).
[24] H. G. Muller, A. Tip, and M. J. Wiel, J. Phys. B: At. Mol. Phys. **16**, L679 (1983).
[25] N. B. Delone, and V. P. Kraĭnov, Phys. Usp. **42**, 669 (1999).
[26] Q. Xie, J. Phys. B: At. Mol. Opt. **42**, 105501 (2009).
[27] M. Chini, X. Wang, Y. Cheng, Y. Wu, D. Zhao, D. A. Telnov, S. Chu, and Z. Chang, Sci. Rep. **3**, 1105 (2013).
[28] S. Chen, M. J. Bell, A. R. Beck, H. Mashiko, M. Wu, A. N. Pfeiffer, M. B. Gaarde, D. M. Neumark, S. R. Leone, and K. J. Schafer, Phys. Rev. A **86**, 063408 (2012).
[29] M. Kalinski, Phys. Rev. A **57**, 2239 (1998).
[30] S. H. Autler and C. H. Townes, Phys. Rev. **100**, 703 (1955).
[31] S. Chen, M. Wu, M. B. Gaarde, and K. J. Schafer, Phys. Rev. A **88**, 033409 (2013).
[32] M. Wu, S. Chen, M. B. Gaarde, and K. J. Schafer, Phys. Rev. A **88**, 043416 (2013).
[33] Q. Z. Hou, W. L. Yang, M. Feng, and C. Y. Chen, Phys. Rev. A **88**, 013807 (2013).
[34] B. Carmeli and D. Chandler, J. Chem. Phys. **82**, 3400 (1985).
[35] J. Dalibard and C. Cohen-Tannoudji, J. Opt. Soc. Am. B **2**, 1707 (1985).
[36] T. Rickes, L. P. Yatsenko, S. Steuerwald, T. Halfmann, B. W. Shore, N. V. Vitanov, and K. Bergmann, J. Chem. Phys. **113**, 534 (2000).
[37] M. Wollenhaupt, A. Präkelt, C. Sarpe-Tudoran, D. Liese, T. Bayer, and T. Baumert, Phys. Rev. A **73**, 063409 (2006).
[38] Y. S. Bai, A. G. Yodh, and T. W. Mossberg, Phys. Rev. Lett. **55**, 1277 (1985).
[39] I. I. Rabi, Phys. Rev. **51**, 652 (1937).
[40] A. Messiah, *Quantum Mechanics* (North-Holland, Amsterdam, 1962).
[41] J. R. Kuklinski, U. Gaubatz, F. T. Hioe, and K. Bergmann, Phys. Rev. A **40**, 6741 (1989).
[42] Ya. B. Zel'dovich, Phys. Usp. **16**, 427 (1973).
[43] K. Bergmann, H. Theuer, and B. W. Shore, Rev. Mod. Phys. **70**, 1003 (1998).
[44] K. Schiessl, E. Persson, A. Scrinzi, and J. Burgdörfer, Phys. Rev. A **74**, 053412 (2006).